Eur. Phys. J. A **19**, 275–282 (2004)
DOI 10.1140/epja/i2003-10118-y

THE EUROPEAN PHYSICAL JOURNAL A

Do we understand the ηN interaction from the near-threshold η photoproduction on the deuteron?

A. Fix[a] and H. Arenhövel[b]

Institut für Kernphysik, Johannes Gutenberg-Universität Mainz, D-55099 Mainz, Germany

Received: 20 June 2003 /
Published online: 23 December 2003 –
Communicated by V. Vento

Abstract. The effects of final-state interaction in incoherent η photoproduction on the deuteron are studied within a three-body approach including a realistic NN potential. The results are compared with available data, and differences with other theoretical predictions are analyzed. The role of the ηN interaction and the possibility of extracting the ηN scattering parameters from this reaction are discussed.

PACS. 13.60.Le Meson production – 21.45.+v Few-body systems – 25.20.Lj Photoproduction reactions

1 Introduction

The role of final-state interaction (FSI) in incoherent photoproduction of η-mesons on the deuteron was investigated in our previous work [1,2]. First, we have considered in [1] the first-order approximation (FOA) where complete hadronic rescattering is included in the two-body subsystems (NN and ηN) only, and in the subsequent work [2] the three-body aspects of the reaction were studied. Summarizing the results we would like to conclude that the importance of final-state interaction arises from two sources which are interrelated. Firstly, the impulse approximation (IA), where the FSI is ignored, predicts a very strong suppression of the cross-section close to the threshold. The reason for this is a strong mismatch between the large nucleon momentum needed for η-meson production (more than 200 MeV/c) and the average available momentum in the deuteron of about 45 MeV/c. The FSI provides an efficient mechanism to compensate this momentum mismatch by the collision between the final particles. As a consequence, already the leading terms in the multiple scattering series associated with pairwise NN and ηN scattering produce a very large enhancement of the η production rate close to the threshold. This conclusion has later been confirmed by Sibirtsev *et al.* [3–5].

The second reason is a relatively strong ηN interaction at low energy. Because of its amplification via the NN interaction, an appreciable attraction in the ηNN system is generated, which in turn leads to a virtual pole in the S-wave part of the three-body scattering amplitude [6–8]. In the case of the spin-singlet ηNN state $(J^\pi, T) = (0^-, 1)$, which dominates the reaction close to the threshold, the pole lies on the three-body unphysical sheet not far from zero kinetic energy [7]. We would like to emphasize that the existence of a virtual state near zero energy is the reason why the FOA cannot provide an accurate description of the reaction dynamics at low energy. This statement is corroborated by the fact that the multiple scattering series converges slowly near the pole so that the FOA does not constitute a reliable approximation to the whole series. In particular, the FOA is unable to account for anomalies in the energy dependence of the total cross-section, since singularities of the three-body scattering amplitude cannot be generated in a perturbative approach (see, *e.g.*, the general arguments given in [9]). Indeed, as was shown in [2], only the full three-body treatment can explain, at least qualitatively, the anomalously strong rise of the experimental $\gamma d \to \eta X$ cross-section just above threshold.

However, our work in [2] was only considered as a first step for taking into account the most important dynamical properties of the ηNN system, because of several simplifications for the two-body forces. This concerns primarily the NN sector, especially the deuteron wave function, which in [2] was taken as a pure $^3S_1$ state, generated by the Yamaguchi potential [10]. Clearly, such a treatment is too simple for η photoproduction where large momentum transfers come into play.

Thus, the first motivation for the present paper is to overcome this shortcoming by using a realistic NN potential. In sect. 2, we give the details of the two-body interactions and present the results for the total and differential cross-sections. For the comparison with the inclusive data of [11] also the coherent reaction $\gamma d \to \eta d$ is calculated.

[a] On leave of absence from Tomsk Polytechnic University, 634034 Tomsk, Russia.
[b] e-mail: arenhoev@kph.uni-mainz.de

As will be shown, our predictions slightly underestimate the data in almost the whole energy region from threshold up to $E_\gamma = 750$ MeV. We will discuss possible reasons for this disagreement. The second motivation of the paper is to compare our results with the work of Sibirtsev *et al.* [3–5]. In sect. 3 we point out the principal disagreements between the results of [3–5] and ours, which cannot be explained by the differences of the model ingredients. Finally, in sect. 4 we analyze the possibility of extracting the strength of the ηN interaction in incoherent η photoproduction on the deuteron.

2 Two-body input and discussion of the results

The transition matrix element of the reaction $\gamma d \to \eta np$ has been evaluated with inclusion of the hadronic interactions between the final particles whereas the initial electromagnetic interaction is treated perturbatively in lowest order. The general formalism of our approach is described in detail in [2]. Here we present mainly the most important two-body ingredients of the calculation.

As a basic input we need the ηN and NN scattering amplitudes which were restricted to S states only in view of the near-threshold region. For the ηN interaction we use a conventional isobar ansatz, as described in detail in [12], where the ηN channel is coupled with πN and $\pi\pi N$ channels through the excitation of the $S_{11}(1535)$ resonance. The separable ηN scattering matrix has the usual isobar form

$$t_{\eta N}(q,q';W) = \frac{g_\eta(q)g_\eta(q')}{W - M_0 - \Sigma_\eta(W) - \Sigma_\pi(W) + \frac{i}{2}\Gamma_{\pi\pi}(W)}\,, \tag{1}$$

as a function of the invariant energy W. The $S_{11}(1535)$ self-energies Σ_η and Σ_π are determined by the vertex functions $g_\alpha(q)$ as

$$\Sigma_\alpha(W) = \frac{1}{(2\pi)^2}\int_0^\infty \frac{q^2\,\mathrm{d}q}{2\omega_\alpha}\,\frac{[g_\alpha(q)]^2}{W - E_N(q) - \omega_\alpha(q) + i\epsilon}\,, \quad \alpha \in \{\pi,\eta\}\,, \tag{2}$$

with E_N and ω_α, ($\alpha \in \{\pi,\eta\}$) denoting the on-shell energies of nucleon and meson, respectively. The two-pion channel is included in a simplified manner by adding the $S_{11} \to \pi\pi N$ decay width, parametrized by

$$\Gamma_{\pi\pi}(W) = \gamma_{\pi\pi}\frac{W - M_N - 2m_\pi}{m_\pi} \quad \text{with} \quad \gamma_{\pi\pi} = 4.3\ \text{MeV}\,. \tag{3}$$

The vertex functions are taken in a Hulthén form,

$$g_\alpha(q) = g_\alpha\left[1 + \frac{q^2}{\beta_\alpha^2}\right]^{-1}, \tag{4}$$

containing the strength of the coupling g_α and the range of the Hulthén form factor β_α. The parameters (see table 1) were adjusted to fit the ηN scattering length

$$a_{\eta N} = (0.5 + i0.32)\ \text{fm}\,, \tag{5}$$

Table 1. Parameters of the ηN scattering matrix in eqs. (1), (2), and (4).

$a_{\eta N}$ (fm)	g_η	β_η (MeV)	$g_\pi/\sqrt{3}$	β_π (MeV)	M_0 (MeV)
$0.25 + i0.16$	1.43	654.3	1.57	379.2	1563
$0.50 + i0.32$	2.00	694.6	1.45	404.5	1598
$0.75 + i0.27$	2.04	1282.6	0.55	888.0	1673

and at the same time to provide a reasonably good description of the reactions $\pi N \to \pi N$ and $\pi N \to \eta N$ (for more details see [13]). We consider this value as an approximate average of the scattering lengths provided by modern ηN scattering analyses (see, *e.g.*, the compilation in table I of [4]). In sect. 4, where we study the dependence of the results on the ηN interaction strength, two other sets of ηN parameters are used. The first one, giving $a_{\eta N} = (0.25 + i0.16)$ fm, is taken from [12]. The second set is adjusted such that the scattering length $a_{\eta N} = (0.75 + i0.27)$ fm of the analysis [14] is reproduced. The corresponding parameters are listed in table 1.

We would like to emphasize that the latter value is obtained simply by varying the parameters of our separable ansatz (1) without using the original model of [14]. One of the consequences of this strategy is that the Born term introduced in [14] is absorbed in our approach by the resonance amplitude, which leads to an overestimation of the S_{11} contribution. In this case, we achieve a satisfactory description of the $\pi N \to \eta N$ experimental cross-section, and the resulting ηN amplitude agrees rather well with the ones of [14]. However, unlike the first two sets, we cannot reproduce the S_{11}-wave of the $\pi N \to \pi N$ analysis [15], also below the ηN threshold, unless a relatively large contribution of the $S_{11}(1650)$ resonance is included.

The electromagnetic vertex of the amplitude $t_{\gamma p}$ for the elementary process $\gamma p \to \eta p$ was fixed by fitting the corresponding data of [16]. Below the ηN threshold, we have required that the pion production amplitude $\gamma p \to S_{11}(1535) \to \pi N$, taken from [17], is reasonably well described as presented in [13]. For the neutron amplitude we have used the relation

$$t_{\gamma n} = -0.82\, t_{\gamma p}\,, \tag{6}$$

which is consistent with the experimental value $\sigma_{\gamma n} = 0.67\sigma_{\gamma p}$ extracted from η photoproduction on very light nuclei [18,19].

With respect to the NN interaction, only the most important $^1S_0$ state is taken into account, since, as was shown in [1], the contribution of the triplet state is insignificant, primarily due to the isovector nature of the electromagnetic excitation $\gamma N \to S_{11}$. For the $^1S_0$ state we have used the separable representation BEST3 [20] for the Bonn potential. The deuteron bound-state wave function was calculated using the corresponding BEST4 version for the $^3S_1 - {}^3D_1$ states.

The three-body integral equations were solved only for the lowest S-wave three-body configuration where the orbital angular momentum $l = 0$ in the two-body

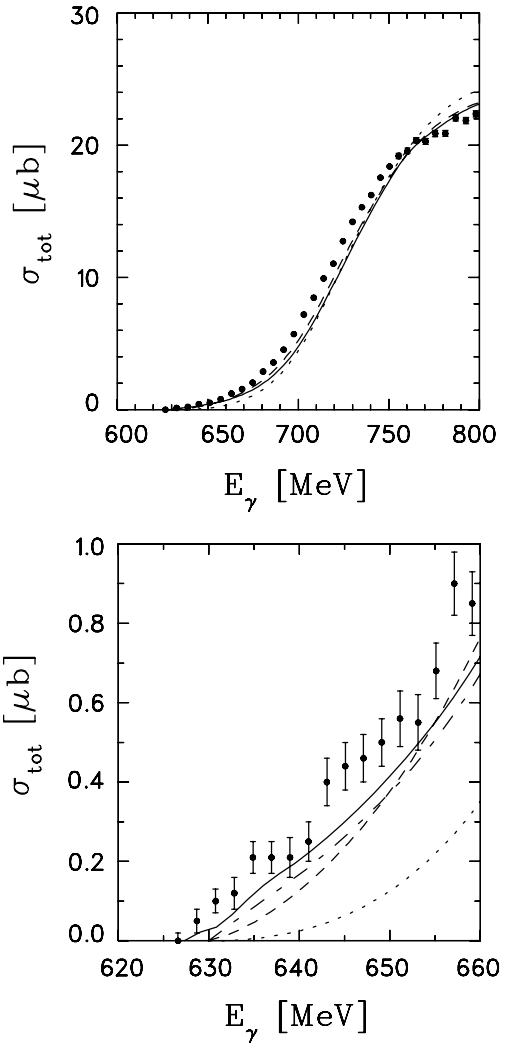

Fig. 1. Total cross-section for the reaction $\gamma d \to \eta np$. The near-threshold region is shown separately in the bottom panel. The dotted, dashed and dash-dotted lines correspond to the impulse approximation (IA), first-order calculation (FOA) and three-body model for the final ηNN state. The inclusive cross-section $\gamma d \to \eta X$, obtained by adding the coherent cross-section (see fig. 3) is shown by the solid curve. The inclusive data are taken from [11]. The dash-dotted and solid curves are indistinguishable in the top panel.

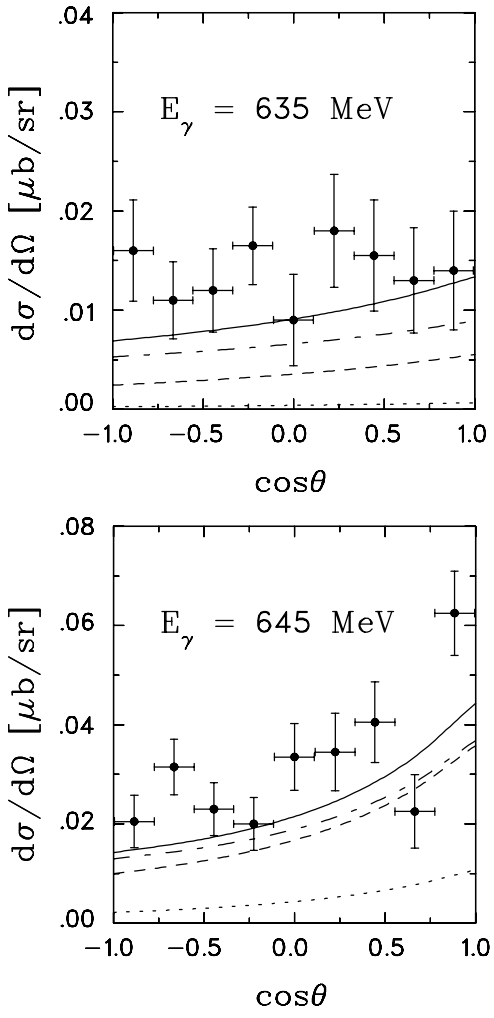

Fig. 2. Differential cross-section for $\gamma d \to \eta np$. Notation as in fig. 1.

subsystems is coupled with angular momentum $l = 0$ of the third particle with respect to the pair. The remaining partial waves were treated perturbatively up to the first order in the S-wave t-matrices of NN and ηN scattering. This approximation is well justified by the strong S-wave dominance in the NN and ηN low-energy interactions. As was shown in [2], it is the lowest S-wave three-body state, that is very sensitive to the higher-order scattering contributions, whereas the higher partial waves are well approximated by the first-order terms. As already indicated above, perturbative calculation, where only pairwise NN and ηN FSIs are taken into account in all partial waves, is referred to as first-order approximation (FOA).

The significance of FSI is demonstrated in fig. 1 for the total cross-section and in fig. 2 for the η angular distribution. In order to appreciate the importance of a realistic treatment of the NN sector, the results should be compared with those presented in figs. 8 and 9 of [2], obtained by means of the Yamaguchi potential and using a pure S-wave deuteron. As expected, for a realistic NN interaction the FSI effect becomes smaller. The obvious reason is the NN-repulsive core which weakens the attraction in the final ηNN system at small relative distances. At the same time the "three-body" effect remains important. For instance, at $E_\gamma = 635$ MeV, the three-body treatment enhances the first-order result by about a factor two. Also, the steep rise right above threshold is a characteristic feature of the three-body approach which is not born out in FOA.

In order to compare our results with the inclusive measurement [11], we calculated in addition to the break-up channel the coherent cross-section $\gamma d \to \eta d$. In analogy with the incoherent process, the calculation was performed within the quasiparticle formalism of the three-body problem, as described in [2]. In this case we neglect the small contribution of the deuteron D state, which contributes only 1% in the IA cross-section. Since

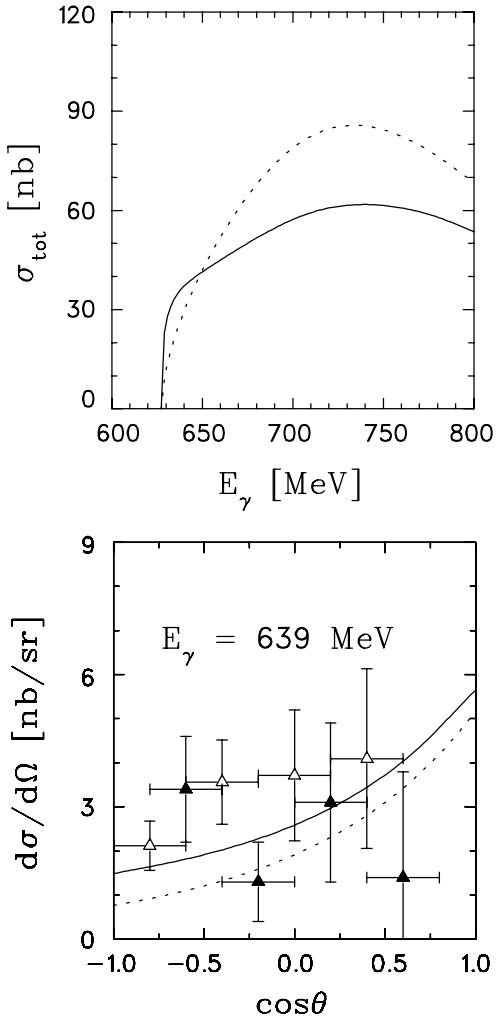

Fig. 3. Total and differential cross-sections for coherent η photoproduction on the deuteron. The IA and three-body results are shown by the dotted and the solid curves, respectively. The data are from [18] (open triangles) and [21] (filled triangles).

the coherent cross-section is proportional to the modulus of the isoscalar part $g_{(s)}$ of the $\gamma N \to S_{11}$ transition amplitude, we have fixed it according to the relation $\alpha = |g_{(s)}|/|g_{\gamma p \to S_{11}}| = 0.25$ as found in [22]. This value is also close to $\alpha = 0.22$ of [12]. The corresponding total cross-section and one angular distribution are plotted in fig. 3. As one can notice, the effect of FSI is also very pronounced. It is not, however, as large as obtained in [2], where we have used a more attractive ηN interaction with $a_{\eta N} = (0.75 + i0.27)$ fm.

Adding the coherent contribution we obtain the inclusive cross-section shown in figs. 1 and 2 by solid curves. We notice that although the three-body calculation leads to a sizable improvement of the theoretical prediction just above threshold, a quantitative agreement with the experimental results has not been reached yet, the theory being too low. Moreover, above $E_\gamma = 650$ MeV the inclusion of higher-order terms in the lowest partial wave acts in the opposite direction by decreasing the cross-section of the FOA. In this region the three-body model exhibits an even larger deviation from the data than the FOA.

The slight disagreement with the experimental results points apparently to the fact that the mechanism of the η photoproduction is more complicated and some of its important details are not properly accounted for by our calculation. In this connection, we would like to make a few comments concerning possible ways of improving the theoretical treatment. The first relates to the off-shell behavior of the ηN scattering matrix, which may be much more complex as given by the vertices $g_\eta(q)$ in (4). In particular, it was already noted in [23] that the simple Hulthén form factors may strongly overestimate the short-range ηNN interaction, since the resulting separable ηN potential is probably too attractive near the origin. This is hardly important for low-energy ηd scattering, but it is relevant for η photoproduction which in general is quite sensitive to the ηN wave function at small distances. Clearly, a more realistic description of this short-range behavior would require a much more thorough treatment of the ηN interaction, where the resonance excitation is considered microscopically with respect to the internal dynamics of hadrons.

Another comment is related to the explicit coupling to πNN states. It was neglected in the present calculation (except for virtual πN decays in the S_{11} propagator), since a correct inclusion of a pion would require substantial refinements of our three-body treatment, in particular the insertion of a variety of resonances which are excited in πN collisions. If the πNN states are properly taken into account, then among other factors the η photoproduction can proceed according to the two-step scheme $\gamma N \to \pi N \to \eta N$, where a pion, being produced by the photon, is subsequently rescattered into an η by the other nucleon. According to the results of [2,22,24], the contribution of the intermediate pion depends strongly on the role of large momentum transfers in the reaction mechanism. For example, whereas πNN states provide only a small fraction of the ηd scattering cross-section [2,24], they contribute rather sizeably to coherent η photoproduction on the deuteron [22]. It was shown in [2], where only the $S_{11}(1535)$ resonance was included into the $\gamma N \to \pi N$ amplitude, that the $\gamma d \to \eta np$ cross-section is insignificantly affected if the pion rescattering mechanism is considered. However, it may well be that inclusion of other resonances into the pion photoproduction amplitude can improve the agreement between our calculation and the data [11].

Finally, it must be noted that the relation (6), fixing the neutron amplitude, is only the simplest variant matching the required relation between the elementary cross-sections. Namely, as was pointed out in [22], it does not account for a possible relative phase between $t_{\gamma p}$ and $t_{\gamma n}$. This phase is predicted, *e.g.*, if the corresponding electromagnetic vertices are extracted by fitting different isotopic channels of pion photoproduction [12,22]. Most likely, this fact is insignificant in the region of large photon energies, where the amplitudes $t_{\gamma p}$ and $t_{\gamma n}$ are added incoherently because of large relative momenta between the particles. At the same time, near threshold the interference between $t_{\gamma p}$ and $t_{\gamma n}$ increases due to a reduction of the available

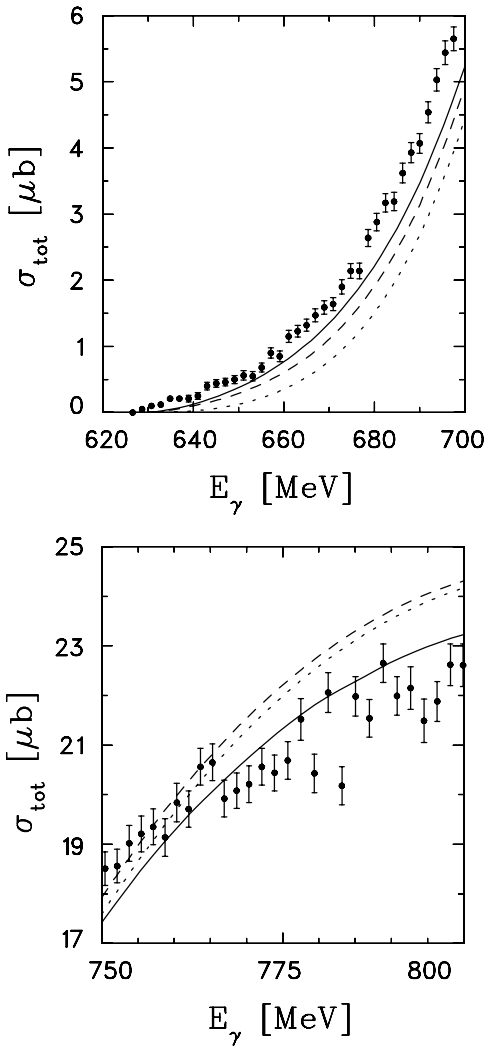

Fig. 4. Total cross-section of $\gamma d \to \eta np$ for two different regions of the photon energy. The dotted curve represents the IA. Successive addition of NN and ηN rescattering in FOA is shown by the dashed and the solid curves, respectively. The $\gamma d \to \eta X$ data are from [11].

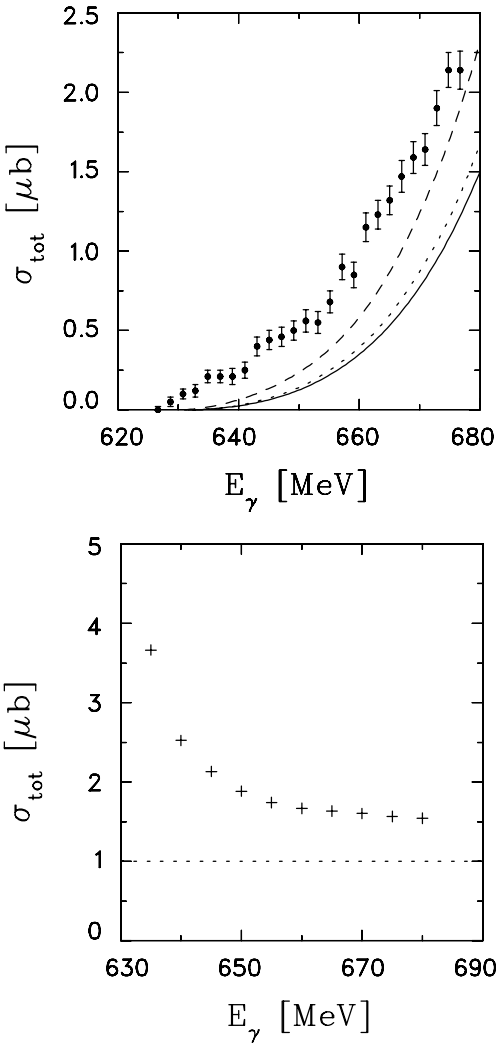

Fig. 5. Top panel: comparison of the IA for the total cross-section from [25] (dotted curve), [5] (dashed curve), and for the present model (solid curve). The $\gamma d \to \eta X$ data are from [11]. Bottom panel: ratio of the IA cross-section of [5] to our calculation.

phase space, which requires a more sophisticated treatment of the isotopic structure of the elementary photoproduction operator.

3 Comparison with other work

Now we turn to the comparison of our results to those obtained by Sibirtsev *et al.* in a series of papers [3–5], where the FSI effects were studied within the first-order approximation. First of all, they confirmed our previous conclusion [1] with respect to the fundamental role of the final-state interaction in the near-threshold region. But moreover, they have claimed that already the incoherent reaction in FOA for the final state without inclusion of the coherent channel provides a good description of the experimental cross-section for $\gamma d \to \eta X$ [11] with a reasonable value for the ηN scattering length. This result is at variance with our own conclusion about the necessity of a three-body treatment of the final ηNN state, and the nonnegligible contribution of the coherent reaction. These contradicting conclusions seem to be especially surprising in view of the fact that the models used in [3–5] and in [1, 2] differ only in nonessential details, such as, *e.g.*, relativistic *vs.* nonrelativistic parametrizations of the η production amplitude. Therefore, we would like to point out the principal discrepancies between our results and those of [3–5] which we were unable to trace back to model differences of the two calculations.

To this end, we show in fig. 4 our first-order calculation of the total cross-section, which reproduces our previous results obtained in [1]. Small deviations are due to different parametrization of the elementary production operator and the ηN scattering amplitude. In the top panel of fig. 5 we compare our impulse approximation (IA) with the corresponding results of fig. 1 in [5] and those presented

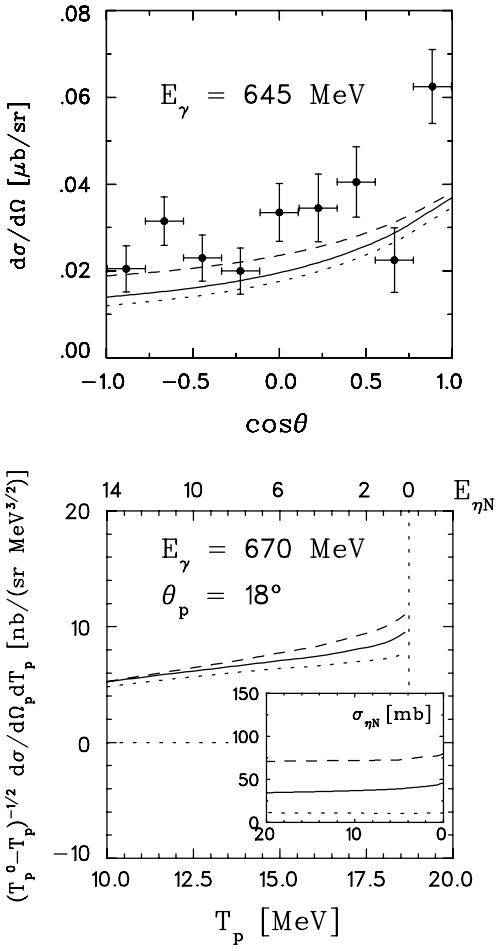

Fig. 6. Top panel: the η angular distribution calculated with different parametrization of the ηN scattering amplitude. Notation of the curves: dotted: $a_{\eta N} = (0.25 + i0.16)$ fm; full: $a_{\eta N} = (0.50 + i0.32)$ fm; dashed: $a_{\eta N} = (0.75 + i0.27)$ fm. The $\gamma d \to \eta X$ data are taken from [11]. Bottom panel: reduced proton energy spectrum, calculated at a fixed angle. Shown is the region in the vicinity of the maximum energy. The internal ηn kinetic energy $E_{\eta N}$ is indicated at the top x-axis. Insert: ηN elastic-scattering cross-section as a function of the energy $E_{\eta N}$. Notation of the curves as in the top panel.

in [25]. The bottom panel shows the ratio of the IA of [5] to our IA. One readily notices that our calculation is in reasonable agreement with that of [25] and the difference of our result to the one of [25] indicates the model dependence to be expected from different parametrization of the elementary photoproduction amplitude and the deuteron wave function. But both IAs are far below the prediction of [5]. For example, at the energy $E_\gamma = 635$ MeV, the latter cross-section is by about a factor 3.6 larger than ours (see bottom panel in fig. 5). This disagreement is especially surprising, since the IA is quite insensitive to the model ingredients. Namely, if one uses a realistic deuteron wave function in conjunction with an elementary production operator fitted to the single nucleon data, than the $\gamma d \to \eta np$ cross-section is fixed almost unambiguously. A little freedom associated with the choice of the invariant energy $W_{\gamma N}$ of the active γN subsystem does not play a role at all, since in the present calculation and in [5] this energy is taken according to the same prescription (compare the formulas (33) of [1] and (2) of [5]). In other words, a model dependence cannot explain such a strong difference between the IA results.

Turning now to the role of FSI, we also find quite different effects. Namely in [5] the FSI effect decreases rapidly above the threshold and vanishes completely at $E_\gamma = 680$ MeV, so that above this point the total cross-section is determined exclusively by the IA, whereas, according to our findings, the FSI contribution does not exactly vanish at all energies examined here. In more detail, the enhancement of the cross-section due to the NN interaction is reduced asymptotically to about 1.5% at $E_\gamma = 780$ MeV (see fig. 4). For the ηN interaction we obtain an enhancement of about 20% at $E_\gamma = 635$ MeV. This effect is visibly smaller than the 45% given in fig. 6 of [4] for the same energy [26]. This disagreement cannot be traced back to the strength of the ηN interaction because the ηN scattering length $a_{\eta N} = (0.42 + i0.34)$ fm used in [4] is even slightly smaller than our value given in (5). With increasing energy the influence of the ηN FSI changes sign and results, according to our calculation, in a slight reduction of about 4% of the cross-section in the resonance peak (see bottom panel of fig. 4). The latter effect must originate from a relatively strong absorption of η-mesons through the rescattering into pions, which is expected to be most pronounced in the resonance region. The same smearing of the resonance peak due to the strong inelasticity of the ηN interaction is observed also in heavier nuclei [27], where it manifests itself naturally much stronger. This energy dependence of the ηN FSI is not supported by the results presented in [4,5], where rescattering effects do not play any role above $E_\gamma = 680$ MeV. We would like to point out that this discrepancy must be explained before any conclusion about the understanding of η photoproduction on the deuteron is drawn.

4 The role of the ηN interaction

In this last section we address the question as to what extent the ηN interaction can be "extracted" from incoherent η photoproduction on the deuteron. The idea to obtain the information on the ηN low-energy scattering parameters from this reaction was explored in [4,5]. In particular, it was found that the cross-section is quite sensitive to the ηN interaction strength, making it possible to study ηN scattering by analyzing the observed single-particle spectra or angular distributions.

In our opinion, such a method very likely will meet with serious difficulties, and we support our scepticism by several numerical results presented below. Firstly, and this is the crucial point for the following conclusions, we do not observe any strong sensitivity of the cross-section to the ηN interaction strength as is claimed in [4]. The effect on the η angular distribution of varying the ηN parameters is demonstrated in the top panel of fig. 6. The calculations are performed within the three-body approach as outlined

above. In each case the e.m. vertex was adjusted to reproduce the elementary experimental cross-section. Comparing the present result with fig. 4 of [5], one sees that in our case the dependence on the ηN scattering length is much less pronounced. Thus, we have to conclude that the experimental discrimination between different ηN models would require extremely precise measurements.

Furthermore, such a weak sensitivity makes the extraction of the ηN scattering parameters very model dependent. The reason has to do with the off-shell behavior of the $\gamma N \to \eta N$ amplitude. This is especially critical for the region below the free ηN threshold which comes into play, when contributions beyond the IA are considered. For example, the results presented above are obtained within the so-called "spectator on-shell" choice for the invariant energy $W_{\gamma N}$ of the γN system, which is natural for the nonrelativistic three-body theory. In this case, as one integrates over the spectator nucleon momentum in the deuteron, $W_{\gamma N}$ covers the range $[-\infty, W - M_N]$, where W is the invariant energy of the ηNN system. Although the uncertainty of the $\gamma N \to \eta N$ subthreshold behavior is not very crucial for the incoherent reaction, it makes the method of precise determination of ηN parameters much more ambiguous than was presented in [4]. This difficulty is quite general when one tries to determine the contribution of an individual diagram to the whole amplitude.

In this connection we would like to recall the Migdal-Watson theory [28,29] which makes it possible to study the two-body interaction without regard to the particular way of embedding this interaction into the reaction amplitude. According to this theory, the low-energy parameters of two-body scattering can in principle be identified by fitting the energy spectrum of the third particle close to the maximum energy value. In order to illustrate the practical applicability of this method to the ηN interaction, we show in the bottom panel of fig. 6 the proton spectrum at a fixed angle $\theta_p = 18^\circ$. The curves were obtained within the three-body approach using the same three different parametrizations of the ηN sector as in the top panel. Only the upper end of the spectrum, corresponding to low relative ηn energies, is shown, since only this part is relevant. According to the Migdal-Watson theory, the behavior of the proton energy distribution in this region reflects the energy dependence of the elementary ηn cross-section, disregarding the terms which depend weakly on the ηn relative energy. To eliminate the effect of the kinematical boundary, the spectrum is divided by $(T_p^0 - T_p)^{1/2}$, where T_p^0 is the maximum proton energy. As one can note, also in this case the experimental discrimination between the ηN models seems to meet with the same difficulties. Namely, the form of the spectrum is not strongly affected by the ηN interaction. The reason is that the form of the ηN elastic-scattering cross-section, shown in the insert in the bottom panel, does not sizeably vary with the value of $a_{\eta N}$.

5 Conclusion

The role of final-state interaction in incoherent η photoproduction on a deuteron has been investigated using a three-body model for treating the interaction in the final ηNN system. In contrast to our previous work [2] the present results were obtained by using a realistic NN interaction based on the separable representation of the Bonn potential. As a summary, we would like to draw the following conclusions:

i) As may be expected, a realistic treatment of the NN sector reduces the FSI effect compared to the use of a simple Yamaguchi potential. At the same time, the influence of higher-order rescattering in the final state remains essential and must be taken into account close to the threshold.

ii) Our three-body calculation underestimates the data [11] slightly in the energy region up to $E_\gamma = 780$ MeV. One open point, which remains to be investigated in this connection, is the short-range part of the ηNN wave function. The latter can be quite sensitive, *e.g.*, to the contribution of the πNN configuration which was omitted here.

iii) There exists a principal discrepancy between our results and the ones of Sibirtsev *et al.* [3–5]. Most disturbing is the fact that already the simple impulse approximation of [3–5], where the model ambiguities should be small, exhibits a strong disagreement with other authors [1,25]. In this connection we would like to emphasize that the statement that the reaction $\gamma d \to \eta np$ is well understood within existing theoretical approaches is premature, even if a seemingly good description of the data in [5] is achieved. Further theoretical work is certainly needed.

iv) We do not find a strong sensitivity of the $\gamma d \to \eta np$ cross-section to the ηN interaction strength as was claimed in [4]. Our calculation shows that even if the off-shell uncertainty of the $\gamma N \to \eta N$ amplitude is disregarded, quite a weak dependence of the results on the ηN interaction parameters renders a precise determination of the ηN interaction practically impossible.

The work was supported by the Deutsche Forschungsgemeinschaft (SFB 443).

References

1. A. Fix, H. Arenhövel, Z. Phys. A **359**, 427 (1997).
2. A. Fix, H. Arenhövel, Nucl. Phys. A **697**, 277 (2002); Phys. Lett. B **492**, 32 (2000).
3. A. Sibirtsev *et al.*, Phys. Rev. C **64**, 024006 (2001).
4. A. Sibirtsev *et al.*, Phys. Rev. C **65**, 044007 (2002).
5. A. Sibirtsev *et al.*, Phys. Rev. C **65**, 067002 (2002).
6. A. Deloff, Phys. Rev. C **61**, 024004 (2000).
7. A. Fix, H. Arenhövel, Eur. Phys. J. A **9**, 119 (2000).
8. S. Wycech, A.M. Green, Phys. Rev. C **64**, 045206 (2001).
9. C. Goebel, Phys. Rev. Lett. **13**, 143 (1964).
10. Y. Yamaguchi, Phys. Rev. **95**, 1628 (1954).
11. V. Hejny *et al.*, Eur. Phys. J. A **13**, 493 (2002).
12. C. Bennhold, H. Tanabe, Nucl. Phys. A **530**, 62 (1991).
13. A. Fix, H. Arenhövel, nucl-th/0302050.
14. A.M. Green, S. Wycech, Phys. Rev. C **55**, 2167 (1997).
15. R.A. Arndt, J.M. Ford, L.D. Roper, Phys. Rev. D **32**, 1085 (1985).

16. B. Krusche *et al.*, Phys. Rev. Lett. **74**, 3736 (1995).
17. D. Drechsel, O. Hanstein, S.S. Kamalov, L. Tiator, Nucl. Phys. A **645**, 145 (1999).
18. P. Hoffmann-Rothe *et al.*, Phys. Rev. Lett. **78**, 4697 (1997).
19. J. Weiss *et al.*, Eur. Phys. J. A **16**, 275 (2003).
20. J. Haidenbauer, Y. Koike, W. Plessas, Phys. Rev. C **33**, 439 (1986).
21. J. Weiss *et al.*, Eur. Phys. J. A **11**, 371 (2001).
22. F. Ritz, H. Arenhövel, Phys. Rev. C **64**, 034005 (2001).
23. G. Fäldt, C. Wilkin, Phys. Scr. **64**, 427 (2001).
24. H. Garcilazo, M.T. Peña, Phys. Rev. C **66**, 034606 (2002).
25. C. Sauermann, PhD Thesis, Technische Universität Darmstadt (1996) (`http://theory.gsi.de/the/the_diss.html`); C. Sauermann, B. Friman, W. Nörenberg, Phys. Lett. B **409**, 51 (1997).
26. There is an inconsistency to the interaction effect shown in fig. 5 of [4], where the ηN enhancement is even larger, namely more than 100% at $E_\gamma = 635$ MeV.
27. M. Roebig-Landau *et al.*, Phys. Lett. B **373**, 45 (1996).
28. A.B. Migdal, *Qualitative Methods in Quantum Theory* (Benjamin, Reading, 1977).
29. K.M. Watson, Phys. Rev. **88**, 1163 (1952).